

Nuclear Waste Burnup Using a Dust Reactor

George Chapline, Rodney L. Clark² and Robert B. Sheldon³
Grassmere Dynamics LLC, 774 Bob Stiles Rd, Gurley, AL, 35748, USA
NASA/MSFC/NSSTC/SP62, Huntsville, AL, 35805, USA

1 Introduction

We are currently pursuing a novel concept for using a dust reactor to burn-up in situ the spent nuclear fuel currently being stored at nuclear power stations. In our scheme the spent fuel rods are simply placed inside the reactor; there is no need for reprocessing the spent fuel. The cooling system required by our burn-up scheme is much simpler than in fast breeder reactors, and compared to a conventional light water reactor the cooling requirements are reduced by approximately 50%. In addition, there is no need for a large auxiliary power source as in hybrid magnetic or inertial confinement fusion schemes. Thus the footprint for the dust reactor is relatively small, which would allow this type of reactor to be located on the existing sites of most currently operating commercial nuclear power plants. In the course of burning up spent fuel each of our dust reactors would produce almost 500MW, and so the use of this type of reactor to burn-up spent fuel could eventually eliminate the need to build new light water reactors. There is a residual waste stream, but the volume of this waste stream is much smaller than for convention reactors, and the actinides are almost completely eliminated from the waste.

The dust reactor concept was introduced some time ago by one of us (RC) [1], and is based on the earlier fission fragment (FF) rocket idea [2,3]. The dust reactor would operate as a thermal neutron reactor and use as fuel micron sized pellets of UC. In the FF rocket scheme it was contemplated that the FFs produced in the low density reactor core would be guided out of the reactor core by large magnetic fields. In our nuclear burn-up scheme (see Fig 1) ~ 50% of the FFs produced in the UC fuel could be collected outside the core and as a bonus the energy of these FFs could be directly converted into high voltage electricity.

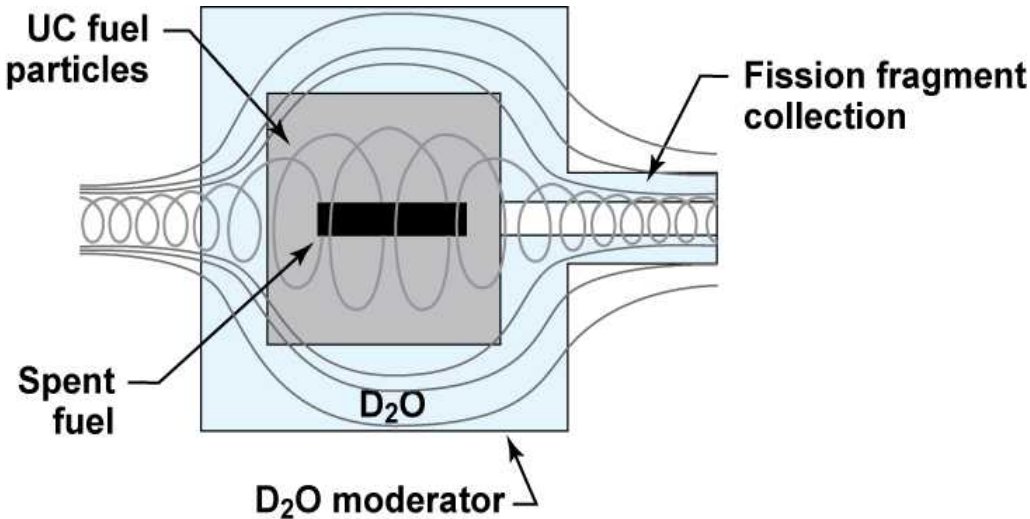


Fig. 1 Scheme for using a dust reactor to burn-up spent fuel

Our concept takes advantage of the fact that the possibilities and limitations for generating self-sustaining fission are

²CEO and founder, Grassmere Dynamics LLC, Gurley AL,35748 Grassmare1@aol.com

³Physicist, NASA/MSFC/NSSTC/SD62, 320 Sparkman Dr Huntsville AL 35805 Rob.Sheldon@msfc.nasa.gov

generally well understood. In particular, we can with high confidence predict what the fuel and cooling requirements are to make a dust reactor work as advertised. We can also accurately predict what the effect would be if, e.g 1 ton, of spent nuclear fuel were placed inside the dust reactor. Of course, whether one could suspend a critical mass of micron sized UC fuel particles inside the reactor core is a novel question that would require considerable further research.

Although we have already 10 years ago estimated the critical masses of Pu239 and U235 required for the fission fragment rocket, we show in Table 1 some recent results for the critical masses of U235 calculated using the Los Alamos Monte Carlo neutron transport code MCNP. The fuel was assumed uniformly fill a cylinder in the chemical form UD or UC, and the moderator was chosen to be either deuterated polyethylene or heavy water.

Table 1

Fuel	Moderator	Fuel dimensions	Average fuel density	Critical mass
UD	110 cm CD ₂	4 m x 5 m	0.2 mg/cm ³	12 kg
UD	250 cm CD ₂	6 m x 5 m	0.1 mg/cm ³	14 kg
UC	200 cm D ₂ O	6 m x 5 m	0.1 mg/cm ³	14 kg

The last line in Table 1 is our “baseline” configuration. The critical masses listed in Table 1 are not very sensitive to the exact distribution of fuel within the reactor core. However, if the dust suspension system fails and the dust falls to the bottom of the core, the reactor becomes sub-critical. In the configuration where the dust fuel is uniformly distributed inside the moderator approximately 50% of the fission fragments produced in the dust escape from the core. The magnetic rigidity Br of fission fragments is ~ 0.6 T-m; therefore most of the fission fragments can be confined within the moderator if the magnetic field varies from about 0.5 Tesla along the central axis to about 2 Tesla at the edge of the fuel. We imagine that the fission fragments being guided from the core by the magnetic mirror can be continuously collected outside the reactor core as indicated in Fig. 1. Because of the very small size of the fuel particles, the energy deposited in the fuel particles by FFs can be radiated away if the reactor power is not too high. We contemplate operating with a reactor core temperature of 1000 K and a “thermal” power (including spent fuel) ~500 MW, which would allow passive radiative cooling of the dusty part of the core.

From the point of view of nuclear waste burn-up the most interesting property of the dust reactor is the separation of the fuel required for criticality and the spent fuel. Both the criticality and breeding of Pu are maintained by slow neutrons. However the power that can be generated is limited by the requirement of radiative cooling for the UC dust; the power generated in the dust must be less than approximately 200 MW. This limits the slow neutron flux in the reactor core to ~ 6x10¹⁴ neutrons/cm²-sec. The Pu breeding is limited by the critical mass of U235 and the mass of U238 in the spent fuel. Assuming the critical U235 mass is 14 kg and the spent fuel contains 1 ton of U238, the equilibrium Pu inventory is 15 kg (the initial Pu content of the spent fuel is about 8 kg per ton of spent fuel). Thus the power by the Pu will always be comparable to but somewhat larger than the power generated by the U235. The U238 in the spent fuel will be slowly consumed by the Pu breeding (the consumption by fast neutron fission is much smaller); for a reactor power of 500 MW essentially all the actinides in the spent fuel will be consumed in 20 years.

Proof of Principle Experiments

Dusty plasmas are of great interest in astrophysical contexts and for semiconductor processing. In fact the dusty plasmas we require for our reactor core are not very different from the dusty plasmas commonly used for plasma etching in the semiconductor chip industry. These plasma etching machines typically use 2 μm diameter SiO₂ particles with a density of 10⁸ particles per cc. Remarkably, this is essentially identical with our standard model for

the reactor core, which would use $\sim 1 \mu\text{m}$ diameter UC particles with a density $\sim 10^8$ particles per cm^{-3} .

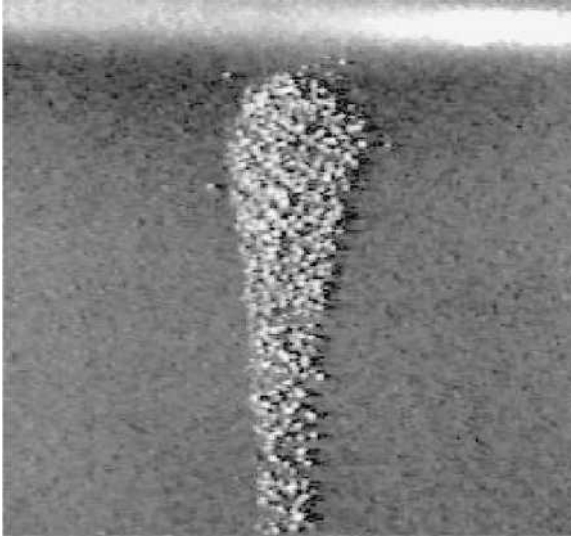


Fig. 2 Suspended micron size CeO_2 particles

We contemplate that the fuel particles in our reactor core can be kept levitated using electrostatic fields. Experiments demonstrating this possibility using micron sized CeO_2 particles have been carried out at the High Energy Density Research Center in Russia [4] In Fig. 2 we a picture of the suspended CeO_2 particles in the Russian experiments where the CeO_2 particles have become charged as a result of exposure to a $\text{Cf}252$ spontaneous fission source. The particles are kept apart by their mutual electrostatic repulsion.

As a first step towards evaluating the feasibility of suspending a critical mass of micron sized UC particles in a vacuum, it will be necessary to understand how the emission of fission fragments and exposure to fission gamma rays in the presence of a hydrogen plasma affects their charge state. As a first experiment we propose measuring the equilibrium charge of an Am or Cf grain suspended in a Paul trap in the presence of a gamma source. Once the charging of micron sized fuel particles is understood, we can proceed to design a prototype dusty reactor neutron source.

2 Technological Hurdles of Present Designs

Problem of Fusion Heating

In 1979, Hans Bethe published a report on how to burn up used fuel rods with a fusion reactor although no fusion experiment had come close to breakeven, but in the intervening 30 years, two fusion technologies have matured: inertial confinement, and magnetic confinement. Physics Today [4] carries schematics of the three leading designs for a hybrid reactor: two magnetic confinement tokomaks with the fissile blanket either inside or outside the magnet coils, and an inertial confinement laser fusion device with the blanket external to the device. In all three cases, there is some concern that scaling the power from laboratory testing (pulsing once every several hours) to commercial production (pulsing 10 times a second) will be a serious technological hurdle.

A third fusion technology deserves mention because of its relevance to fissile feedback, and that is electric (rather than magnetic) confinement epitomized by the Farnsworth-Hirsch "fusor"[6]. Advances in fusor technology have replaced the simple electrodes with magnetically coils, producing a non-neutral plasma (electrostatic) confinement for the D-T plasma[7]. Despite these real advances, the radiative losses most likely exceed the heating rate, so like the other fusion sources, the heating needed for scaling up to commercial production remains a technological hurdle.

Problem of Fission Heating

While the difficulties of fusion power are well known, Bethe discusses the technological hurdles of the fissile design, whose heating rate is proportional to the neutron density. Since most of the current fusion devices are pulsed, the heating rates are also pulsed, with peak powers sufficient to vaporize the fissile fuel. Bethe writes,

When I first wrote about the fusion hybrid I found it very difficult to estimate its cost. But now the work of the Argonne group has given a reasonable basis for an estimate. They argue that the main cost is related to the removal of heat, and should therefore be proportional to the total thermal power. Furthermore, since heat removal from the blanket is likely to be complicated, they take the cost per unit power to be the same as for the fast breeder reactor[4].

That is to say, nearly all of the fission reactors are designed to provide steady-state power, whereas nearly all the fusion reactors are designed for pulsed power. Therefore adapting current fission designs to a fusion reactor will require careful attention to the pulsating heat load expected.

2.1 Feasibility of the Dust Based Fission Fragment Reactor

We think that both the problem of higher power / repetition rates and the problem of dissipating pulsed peak heat can be addressed with the use of a dusty plasma fissile feedback in a way that both simplifies the design and increases the efficiency of the fusion reactor.

Solution for Pulsed Fissile Heating

The cause of the excess heat is not the kinetic energy of the neutron stopping in the fissile dust, nor even the radiant energy released in the neutron-initiated fission. Rather, the heat comes about by the frictional stopping of the resultant fission fragments (FF) within the fissile fuel. Should this frictional heat input raise the temperature of the fissile fuel too high, the fuel would melt and vaporize, causing the sorts of problems observed at the Three-mile Island or the Chernobyl nuclear plant.

But by dividing the fuel into micron-sized grains, the fuel can radiatively cool down to safe temperatures even while undergoing the same frictional heat load. In addition, the FF can escape from the micron-sized fuel with minimal frictional heating, which also reduces the heat load. Both radiative and frictional heat loads are then transferred to the walls of the dusty plasma chamber, which can be made much larger in area and more massive than the fissile dust itself, thereby separating the heat absorber from the heat producer. Figure 2 shows the temperature range expected for two sizes of dust grains at different power loads of a dusty plasma device.

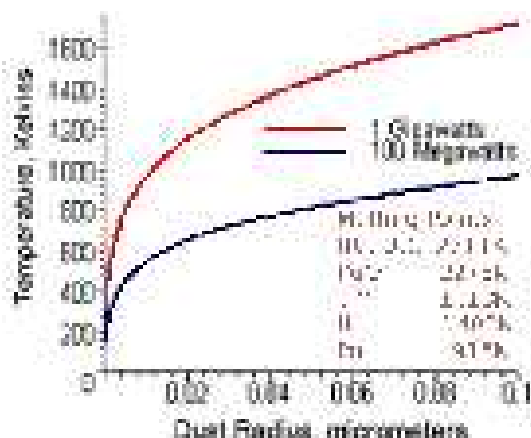


Figure 2: Equilibrium fuel particle temperature as a function of particle size for two power levels.

Solution for Fusion Pellet/Plasma Heating

An additional benefit is gained if the dusty plasma fissile fuel is embedded in a very high magnetic field. The magnetic field confines and delimits the dusty plasma, while the FF can then be extracted and focussed by the multi-

Tesla magnetic fields, so as to provide particle beam heating of the D-T pellet/plasma. The advantage over other heating methods lies in the power density of the FF beam, which can be up to MW of continuous power in relatively small area. The feedback between the fusion heating and the intensity of the beam is positive, with several FF produced for every neutron released by fusion, and proceeds at lightspeed with microsecond reaction time, providing the burst of GW power needed for millisecond rep rates.

Since the FF beam is extracted magnetically, it is physically separate from the fusion device. We sketch two possible arrangements of the fissile feedback and the fusion reactor. In panel a) of Figure 3 we superpose a dipole field from a superconducting coil on a spherical fusion geometry, which can be an inertial fusion or an electrostatic fusion device, illustrating how magnetic fields can redirect FF into the fusion core. This use of a dipole field to trap and heat a fusion plasma is being studied with the Columbia/MIT levitated superconducting dipole fusion device. [8]. Alternatively, a cylindrical magnetic field can be used to focus opposing FF beams into a magnetically confined plasma, illustrated schematically in panel b) with a magnetic mirror fusion device.

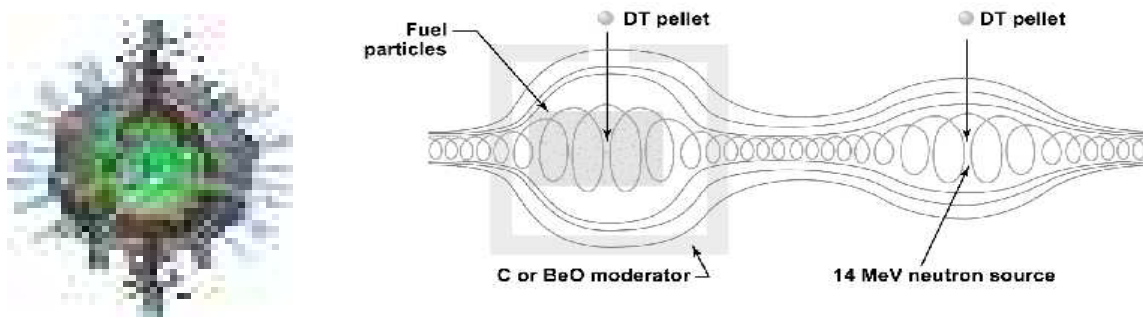


Figure 3: Schematic fusion heating from fissile feedback in a) dipole magnetic geometry, and b) cylindrical magnetic geometry.

Therefore dusty-plasma fissile feedback can solve the problem of heating the fusion reactor in the millisecond timescales needed for a commercial pulsing rate without simultaneously overheating the fissile fuel. This greatly simplifies the design and reduces the technological hurdles of a fusion reactor while permitting the high neutron fluxes needed to rejuvenate/burn spent fuel rods.

2.2 Sub-critical Dusty Plasma Fission Development

In the previous section, we introduced the basic concept for the development of a fusion reactor with dusty plasma fissile feedback. A preliminary step before closing the loop is the technological development of a sub-critical dusty plasma fission module. That is, the dusty plasma module can be developed and validated with neutrons from any source, whether from a fusion device or a test reactor. Therefore we define the experimental requirements of a sub-critical dusty plasma fission device, where the fuel consists of a cloud of nano-particle dust (~ 1000 nm diameter) composed of fissile material, which allows the FF to escape from the fuel particles with a high probability, while the large surface to volume ratio of the fuel particles enables them to radiate heat effectively to the walls.

The fuel particles in the core of the reactor form a dusty plasma cloud, which must be confined away from the walls while the FF are extracted. This can be accomplished using the significant difference in both the energy per charge and the mass per charge ratios between the fuel particles ($E/q = 10\text{eV}/q$, 10 amu/e) and the FF ($E/q = 10\text{eV}/q$, 5 amu/e), which allows the fissile dust to be electrostatically or magnetically contained within the reactor core while the more energetic FF are extracted for power, thrust, or heating. The stream of FF, carrying most of the energy, is composed of positive ions that can either be used as rocket exhaust, a high voltage dc power supply with 90% efficiency[9], or as a heating source for D-T fusion.

Neutronic Analysis

A neutronic analysis has been performed using standard codes[10], where a dusty plasma fuel is homogeneous from the neutron's point of view, since the mean free path of the neutron is very long in this low density fuel. Therefore

after a fission generates a neutron, it exits the dusty core and is thermalized in the moderator, entering and reentering the core many times before it is finally absorbed. The low density, however, necessitates a highly efficient moderator, which we model as deuterated C-polyethylene. Table 1 lists the critical mass of U235 for several different density dusty plasma cores. From the point of view of extracting a FF beam, the density should not go above about 0.1 mg/cc, which also gives the largest volume. Should the size be a problem, we have investigated several other isotopes with higher cross-sections that reduce the critical mass, with Pu239 at 50% and Cm245 at 10% of the size of a U235 reactor.

Table 1: Critical mass for several dusty plasma configurations

Fuel	Moderator thick (cm)	D x L (m)	density (mg/cc)	Crit. mass (kg)
U235	50	1 x 5	3	11
U235	110	4 x 5	0.2	12
U235	110	6 x 5	0.1	14

If the fissile fuel is fabricated as 4 micron diameter particles, then 90% of the fission fragments will escape from the particle in which they are produced. The density of these dust particles will be determined by the critical mass, which is approximately 15 kg in the case of UC. If the particles are confined in a cylindrical reactor core that is 3.5 meters across and 5 meters long, then the density of fuel particles will be $\sim 5 \times 10^6 / \text{cc}$ and the range of the fission fragments within the reactor core would be ~ 1 m. This should be sufficient to allow roughly 50% of the fission fragment energy to be available for the heating of DT gas inside and surrounding the reactor core.

Dust Density and Volume

Laboratory RF-discharge dusty plasma chambers currently are producing this dust density[11], and we expect that self-ionizing dusty plasmas can sustain even higher dust densities [12]. Although laboratory dusty-plasmas have the required density, none have the required volume. Are there limitations due to longer wavelength instabilities? We do not think so, since polar mesospheric clouds made of ~ 1 micron ice grains form at the 80 km high summer mesopause in layers measured to be ~ 1 km thick with ~ 1 cm structure (unpublished manuscript, Sheldon and Voss, 2006). While one might expect the Rayleigh-Taylor convective mode to destabilize these dust clouds on timescales of a few seconds, the magnetic field provides a much higher rigidity restoring force, so that 5 cm diameter magnetically suspended dust clouds in the laboratory were stable on the order of hours (see Figure 4)[13].



Figure 4: Non-neutral plasma confinement of a dusty plasma cloud.

Thermal Management

The dust in the reactor becomes hot from a small percentage of the FF captured before leaving the fuel particles and because some escaped FF will recollide with the particles. We model this as a fixed percentage of the total power released by the fission process. In equilibrium, this rate of heating is balanced by radiative cooling as described by the Stefan-Boltzmann law. Since the heating is roughly a function of volume, while the cooling is a function of area, the smaller the size of the fuel particle, the cooler the dust at a fixed power level. If we assume the chamber walls are kept cool so that they are a radiative energy sink, then the equilibrium fuel temperature as a function of dust particle size is well below the melting point for several nuclear fuel candidates, as shown in Figure 2.

If the DT is injected into the reactor core as a solid pellet or STP gas, then in a time on the order of a second the DT will be heated to a point where its temperature begins to “run away”. The resulting pulse of 14 MeV fusion neutrons will then induce an intense millisecond pulse of fission fragments which can be used to heat DT in an adjacent magnetic mirror (see Figure 3).

A reactor power of 100 MW is well within the temperature limits that would allow passive steady state radiative cooling of the reactor core and moderator. Turning the reactor on and off in a reactor control period would possibly allow transient powers as high as ~ 1 GW. At a reactor power of 100 MW one could heat 1 gm of DT to a temperature > 1 keV in a second, at which point the temperature of the DT will “run away” due to boosting of the fission rate by the 14 MeV neutrons and self-heating of the DT by alpha particles. Some selected values for the initial FF heating for a 100 MW reactor, boosted FF heating, alpha particle heating, and bremsstrahlung energy loss from the hot DT for a 4 m x 5 m magnetic trap are given in Table 2.

Table 2: Heating/cooling rates for dusty plasma reactor.

T (keV)	Initial FF (MW)	Boosted FF (MW)	Alphas (MW)	Brems. (MW)
1	45	75	0.7	-4.8
2	45	1100	30	-6.8
4	45	36000	1000	-9.6

These numbers assume that all the energy of the fission fragments that escape the reactor core go into heating the DT. In practice it might be necessary to operate at pulsed reactor powers exceeding 100 MW. Although detailed calculations of the DT heating and hydrodynamics remain to be carried out, it appears from the numbers given in Table 2 that in less than a second a 1 gm DT pellet injected into the reactor core can be heated to the point where its temperature “runs away” with a dramatic increase in the fusion rate. Once the temperature of the DT gas exceeds a few keV, it can no longer be confined in the magnet trap for more than about a millisecond. Even so we expect that the millisecond burst of neutrons will produce an intense pulse of up to 10 fission fragments which can then be used to heat DT in a tandem mirror. Since there is no moderator surrounding the tandem mirror containing only DT, the 14 MeV neutrons produced in this central trap can escape into the surrounding space.

Fission Fragment Escape Probability

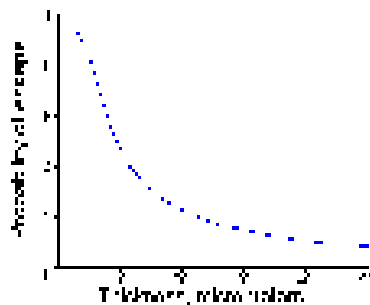


Figure 5: Fission fragment escape probability as a function of fuel particle size.

The FF must escape the dust particle in order to produce usable energy other than heat. The probability for a FF to escape a single dust particle has been calculated in the references and by us. As shown in figure 5, the FF escape probability is very high for small fuel dust particles, reaching nearly 100% for submicron particles.

After escaping the originating fuel, the FF must next escape the dust cloud and the chamber to be useful for thrust, power, or fusion power. This escape probability depends on the trajectory, which without confining magnetic fields, will generally follow a straight-line trajectory. The worst case for heating the fuel is for FF emitted at the center of a homogeneous dust cloud. For a 40 cm thick cloud of 20 cm radius and density of 1×10 grams/cm, the escape probability is 11.4% without a magnetic field. The blue curve in Figure 6b shows the escape probability as a function of emission angle through a homogeneous dust cloud.

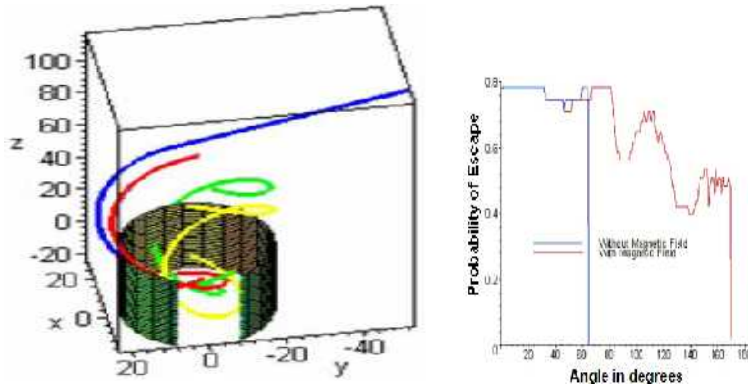


Figure 6: a) Trajectories of FF from dust cloud, which reflect and exit the system. b) Histogram of escape probability for FF as a function of direction and magnetic field.

As expected, only FF emitted in the direction of the beam aperture escape. The situation improves dramatically if a magnetic field is added to guide FF from the device. An axial magnetic field causes FF emitted toward the wall to move in circular trajectories and avoid the wall. And if the magnetic field is stronger at the far end, then it acts as a magnetic mirror reflecting the FF headed in the wrong direction. Figure 6a shows the curved trajectories of four FF as they exit the dust cloud following magnetic field lines. For a 40 cm thick cloud of 20 cm radius, the escape probability is 65% with a magnetic field. The red curve in figure 6b shows the escape probability as a function of emission angle through a homogeneous dust cloud in an axial magnetic field with a magnetic mirror at one end. As expected, additional FF are now redirected through the beam aperture, so that even FF emitted from the center of the dust cloud have a 65% probability of escape.

Magnet Field Extraction of Fission Fragments Exhaust

Table 3: Magnetic properties of fission fragments.

FF label	Atom wt A	MeV/amu E/A	Charge	amu/q A/Z	Speed c	rigidity T-m
Heavy	140	0.5	22	5.9	0.03	0.63
Light	95	1	22	4.3	0.05	0.60
Alpha*	4	1.42	2	0.5	0.05	0.33
Dust	10	10	-100	-10	10	0.001

The next issue is to consider the strength and topology of the magnetic field needed to trap the FF. The radius, ρ in meters, of the circular path taken by a charged particle, Z , in a magnetic field B in Teslas, depends on the atomic number A and the energy E in MeV according to the formula in Tesla-meters. Table 3 shows the magnetic field strength necessary to confine heavy and light fission fragments and alpha particles as a function of these quantities. Field strengths between 0.33 and 0.63 Tesla-meters are required, which can be achieved with water-cooled magnet technology. In order to increase the beam intensity, higher magnetic focussing with super-conducting magnets of one to five Tesla-meter field strengths can be achieved, as is planned for the Auburn University magnetized dusty plasma facility.

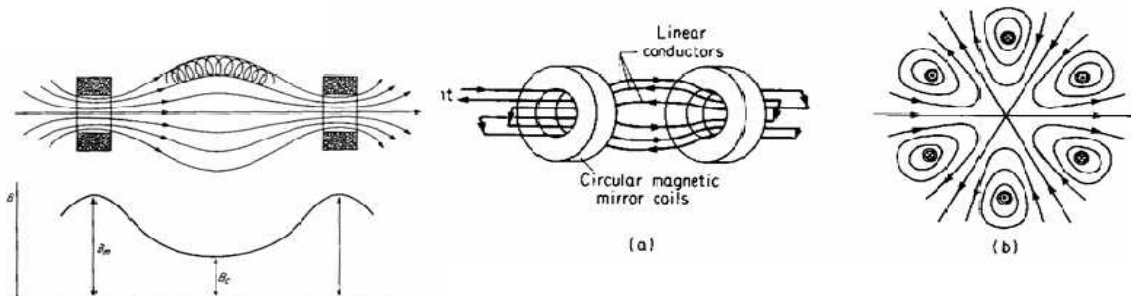


Figure 7: Magnetic confinement of FF in a magnetic mirror. Stronger field on one end reflects FF, weaker field at nozzle transmits FF. Wall fields can be strengthened by multipole fields such as this hexapole current arrangement.

Several magnetic field configurations are possible, the simplest being a magnetic mirror concept as shown in figure 7a. The field strength requirement for a simple coil can be reduced, however, by supplementing with multiple current loops around the perimeter such as the hexapole shown in figure 7b, which can reduce the individual coil strength required by 300%.



Figure 8: Magnetic quadrupole confinement of ion plasma.

The confinement of positive ions by a multipole magnet is demonstrated in Figure 8. A nickel-plated Neodymium-Iron-Boron magnet with surface field approaching 1 T aligned parallel to the cylinder axis was biased to -400V in a 100mTorr atmosphere to produce a dc glow plasma discharge. Electrons emitted from the magnet were ionized air molecules, and the low energy positive ions were then trapped in the strong magnetic field[14]. Two trapping populations were discovered, an outer quasi-dipolar trapping region encircling the ring, and an inner, high-density trap inside the ring. Both the magnetic mirror force, and the geometry of the field lines prevent the positive ion plasma from impacting on the negatively charged magnet, demonstrating confinement of positive ions by multipole magnetic bottle geometry.

Charging of Dust Grains

The fuel particles and the FF in the core of the reactor form a dusty plasma cloud where the small size of the dust grains allows the FF to escape the fuel grains with high probability, leaving the dust charged negatively. The equilibrium charge on the dust can be computed with standard theory[15], which confirms that the large positive charge (+22) carried off by the fission fragments causes the fuel grains to acquire a high negative charge, which allows for the electrostatic containment of the fuel particles. In a dusty plasma equilibrium, this negative charging is balanced by the positive charging from electron emission, both from thermoelectric / photoelectric effects as well as secondary electrons sputtered off the surface by FF collisions. Surprisingly, the models for this process are not confirmed by experiment, which find that the dust charge is a function of many factors: dust particle size, number of +22-charged fission fragments leaving dust, secondary electron production, and FF collisions with dust[16].

Separation between Dust and Fission Fragments

In order to confine the dust and extract the FF, we must discriminate between these two components of a dusty plasma. Fortunately, discrimination between the confined dust and the collimated fission fragments is made possible by the vast disparity between the mass/charge ratio and the velocity. Table 3, shows a comparison between the mass/charge ratio for the fission fragments, alpha particles, and the fuel dust particles. Although the rigidity of the dust appears providentially small, suggesting magnetic confinement, the magnetic force exerted on the dust is still insignificant compared to either collisions or electric forces, so that the dust is not significantly affected by the magnetic field. The electric fields that confine the dust are a product of externally applied fields and internal plasma equilibrium as described by dusty plasma physics. This plasma equilibrium is determined by the density of negative dust, positive ions, electrons, and the plasma currents, which will probably require experimentation to determine precisely. However, we have experimental confirmation of a ~ 5V confinement in a non-neutral DC glow discharge plasma experiment.

Figure 4 shows an example of a dusty plasma with electrostatically confined the dust and magnetically constrained plasma. The purple glow is from a DC glow discharge plasma generated in a 150 mTorr nitrogen atmosphere by applying -400V to a nickel-plated, 1 cm diameter Neodymium-Iron-Boron magnet. The 3 micrometer SiO dust grains in a tray below the magnet are negatively charged by an arc discharge, levitate in a ring around the magnet, and are illuminated with a 532 nm green laser. With fissile dust, the charging occurs naturally without the

need for an arc discharge. The electric field is parallel to the magnetic field lines, so that a vertically oriented magnetic dipole can levitate the dust against the pull of gravity. The MeV fission fragments, however, will not be constrained by the weak dusty plasma electric fields, but will be collimated by the magnetic field. Therefore large difference in E/A for fission fragments and dust, means that the dust can be electrostatically confined while the fission fragments remain magnetically collimated.

3 Physical Constraints

The physics of a sub-critical dusty plasma fission device can be studied in a modular fashion, which in the future can be integrated with a working fusion reactor to minimize the technological barriers to building a complete hybrid reactor. Therefore we propose to develop only a sub-critical dusty plasma fission device, beginning from the dust up.

The problem can be broken down into three subsections: A) the physics of single radioactive dust grains; B) the physics of many radioactive dust grains acting as a dusty plasma; and, C) the physics of magnetically extracting fission fragments from a sub-critical, fissioning dusty plasma.

3.1 Physics of Radioactive Single Dust Grains

Despite thirty years of research into the physics of dust clouds—such as the average charge on the dust grains and the physics of three component plasmas—very little is known about the process that charges dust grains and the conditions under which a dusty plasma remains stable [15]. Dr Mian Abbas et al., have been studying these processes for 10 years at MSFC by trapping single dust grains in Paul trap, and found that many of the theoretical predictions turned out to be false [17]. For example, it was widely believed that dust grains smaller than a micron would be more highly charged by UV, but their experiments showed the opposite effect [18]. Similarly, their experiments on charging of Apollo 11 and 17 lunar dust grains by 25eV electron beam showed that small 0.2-0.3 μ m positively charged grains would generally charge rather than discharge[19]. In addition, they did make the first laboratory measurements on rotation and alignment of the analogs of interstellar dust by radiation pressure, and they observed phenomenon thought to be experimentally or theoretically impossible, that under the laboratory light pressure 0.2 μ m size dust grains can spin at very high rates up to 22000 rot/s [20, 21]. But the physics of discrete radioactive dust grains has not yet been investigated (though there have been experiments on radioactive dust clouds[12]).

It is expected that alpha-particle emission will remove positive charge from the dust grain, charging the grain negative. Likewise spontaneous or stimulated fission will result in the removal of positive charge. The excess electrons will gather on the surface after some delay caused by their diffusion from the interior, where the large electric fields on the surface generated by the curvature of the grain will eventually lead to spontaneous electron emission, saturating the negative charge on the dust grain. Both UV and gamma radiation, as well heat will also increase the electron emission so that in equilibrium, a negative discharge current from a radioactive dust grain will exactly balance the radioactive positive ion decay.

This simple picture has already run into problems, since Abbas et al., report that electron beams charge (rather than discharge) positively charged dust grains to positive equilibrium surface potentials depending on the particle size and incident electron energy. It may be that the curvature of small grains is so large that the electron emission rate overwhelms the effect of electron beam charging leading to metastable states. Without an empirical or physical model for radioactive charging, it is difficult to extrapolate to the conditions of a fissile blanket, and therefore we need to take data on the equilibrium charge state of radioactive dust to find which mechanism dominates. Either charge state will work for a dusty plasma, as long as the charge state doesn't go to zero.

Therefore we propose to study the physics of individual radioactive dust grains using the NASA/MSFC Dusty Plasma Lab, using several different alpha, beta, and gamma-emitting dust grains of various sizes that will be subjected to heating, UV, and electron beam discharging, so as to develop an equation predicting the equilibrium charge state under the conditions simulating a dusty plasma fission reactor. We also intend to find the optimum grain size for the device, balancing the need to have a high density for sustaining the nuclear reaction, with the need for a low enough density to extract fission fragments efficiently.

The protocols for conducting the experiment using radioactive dust will be described below, but it is expected that the pico-curries of radioactivity involved will be well within the radiation safety guidelines of the lab.

3.2 Physics of Fissile Dusty Plasmas in Strong Magnetic Fields

The second step that needs to be studied, is the collective effects of many dust grains which have to be suspended against the forces of gravity in a dusty plasma. So the physics of a dusty plasma are the physics of a three (not two) component plasma made of charged radioactive dust, positive hydrogen ions, and negative electrons, which in most cases is also a weakly ionized plasma where the background neutral gas is far more abundant than the ions and electrons.

Ionization

Now in a weakly ionized plasma, there is a constant neutralization from bombarding neutral atoms, wherein electrons recombine with the ions and the system becomes neutral again. So in order to maintain the dusty plasma for any length of time, some process has to continually ionize the neutral gas to keep the plasma. Methods that have been used are: AC radio-frequency heating of the electrons that then collide with neutral atoms and ionize them; DC glow discharge plasmas that make an avalanching spark in low pressure gas with a constant DC current; hollow-cathode, thermal-emission or tube generated plasmas that make plasma in one location and inject it in another (like the starter in fluorescent lights); and of course, radioactive generation of plasmas.

But the method of making the plasma determines the parameters of the dusty-plasma, so, for example, RF heating produces a high electron temperature and works best in a magnetic field, DC glow discharge operates best at 100mTorr of neutral pressure (the Paschen-point), and radioactive ionization operates best in high density gases (or even higher density liquid hydrogen in bubble chambers). In contrast to all these methods of making a dusty plasma, the fission-dusty-plasma regime is a very low density of neutrals (closer to a vacuum), and a self-ionizing source of dust grains. Since the FF are very effective at ionizing neutrals, the background gas will become the dominant positive ion that neutralizes the negative dust. Hydrogen, helium, nitrogen, argon and xenon are all gases that have been used in dusty plasmas. To a certain extent, it is not the dust that determines the density of the dusty-plasma, but the plasma, so that multiply charged xenon ions may produce a denser dusty-plasma than singly-charged hydrogen. One of the goals of this experiment, will be to find the species, pressure and magnetic field regime that best supports a high density radioactive dusty plasma.

Levitation

The second important property of a dusty plasma, is that it can be levitated against the force of gravity. Four basic processes have been demonstrated in the laboratory that can levitate dusty plasmas: neutral winds, electrostatic levitation, magnetic levitation, and non-neutral plasma trapping.

Neutral wind levitation won't be considered, since we want to operate our dusty plasma in a vacuum so as to maximize the extraction of fission fragments, though in principle if we abandon fission fragment extraction and focus only on the superior cooling efficiency of dust, a system like a gas-core nuclear reactor seeded with dust could be designed. While such a system has some advantages, the much greater advantage of extracting fission fragments and using them to heat the fusion reaction causes us to focus on electrostatic and magnetic levitation alone.

Electric levitation is easy to understand and implement. If the dust is charged negatively then a positively charged plate placed above the dusty plasma with a negatively biased plate below will result in a constant electric field that provides an opposite force to the force of gravity: $F=qE=mg$, where for few micron dust grains and few hundred charges, a typical electric field is 100 V/m. Now plasma is by definition a good conductor, so there will also be a DC current carried by the plasma, which will be proportional to the area of the capacitor. In typical DC glow discharge plasmas, there are typically 100's of milli-amps of current in the levitation circuit for a few square centimeters, which for our several square meter design, would scale up to kiloamps at 100V. And while these 10-100 kWatts of power are a few percent of the megawatt thermal output of the reactor, they are a larger percentage of the particle heating that we are attempting to minimize. That is, the electrical energy goes into Joule heating of the plasma and the dust, which in addition to the nuclear fission heat load must be dissipated by radiation. On the other hand, the electric field can be quickly adjusted to maintain a stable configuration, even should the average charge state of the dust change rapidly, say, during the neutron bombardment burn phase of the fusion pellet. So while we don't anticipate using only electric levitation, it may provide useful for controlling the stability of the dust cloud.

Magnetic levitation of dust has been demonstrated in two geometries, a diverging magnetic field geometry that

takes advantage of the diamagnetic properties of most dust grains [22], and a dipole magnetic field geometry that produces a magnetically trapped plasma, which then traps the charged dust[23]. The key discovery of Sheldon, is that it is not necessary to “magnetize” the dust—a magnetic field large enough to keep the gyroradius of the dust inside the chamber—rather it is sufficient to magnetize the plasma, and let a non-neutral plasma electrostatically trap the dust. Unlike electric levitation, this electrostatic charge is not moving, but is trapped by the magnetic fields, forming a “virtual” electrode.

The virtual electrode of a non-neutral plasma is also the Bussard-Krall improvement to the Farnsworth-Hirsch “fusor” design discussed in the introduction[7], and whose recently funded “Polywell” design has many similarities to ours, excepting the dust. Practically, this means that a water-cooled magnet coil rather than a superconducting magnet is sufficient to trap the dust, because far less B-field is required to magnetize the ions of the virtual electrode than to magnetize the dust. While this approach to levitating dust was first discovered by Sheldon in 2002, the concept of a non-neutral plasma that behaves as a virtual electrode builds on 30 years of research into plasma trapping.

Non-neutral plasma levitation forms an electrostatic trap using magnetic gradients and electrostatic field such as the Malmberg-Penning trap[24, 25, 26]. Three cylindrical electrodes surround an axial magnetic field “bottle” that keeps the plasma radially confined. The outer rings have a potential energy higher than the central ring, causing the ions to mirror back-and-forth inside the bottle. Electrons, however, will be pushed from the center out toward the ends. Thus the trapped plasma will have a net positive charge in the middle, which traps the negatively charged dust. Electrons, which have the same charge as the dust, are more mobile, and therefore “evaporate” from the trap, which increases the density of the dust. From the geometry of the trap, the magnetic field must be arranged vertically so that the resulting static electric field opposes gravity and levitates the dust.

The radial electric field resulting from this non-neutrality causes an ExB rotation of the plasma cloud around the axial magnetic field, called the “dicotron” mode. This motion homogenizes the plasma and should stabilize it against dust-acoustic modes in the dusty plasma. While our experiment is designed to explore only first-order effects, magnetic gradients can further stabilize the plasma through this dicotron motion. So it appears that magnetic fields improve the levitation of dust in two complementary ways, permitting some combination of DC electrostatic levitation and non-neutral plasma confinement.

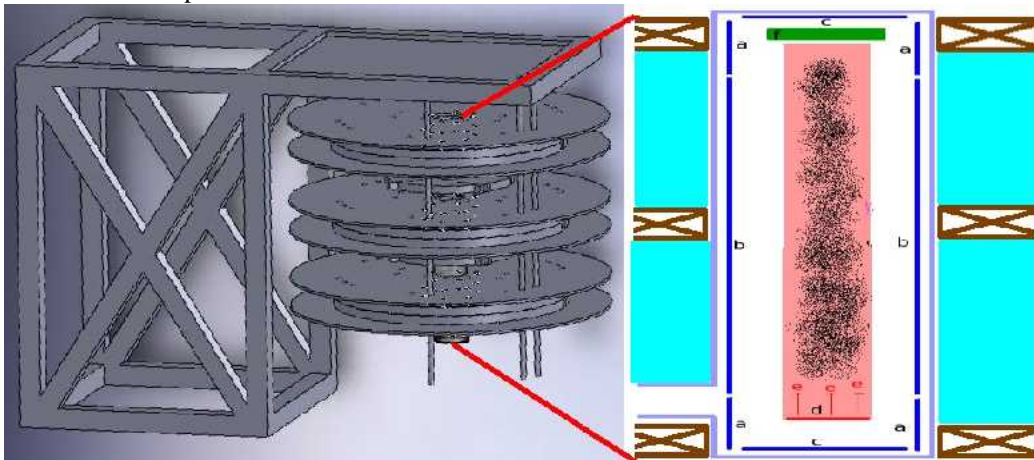


Figure 9: Schematic dusty-plasma levitation test where glass cylinder is enclosed in water-cooled solenoid; electrodes a, b, define a Malmberg trap; electrode c is a levitating capacitor; electrode d is an electron emitter forming non-neutral plasma that holds the dust.

Since non-neutral plasma has never been demonstrated in this geometry, we propose to construct 8cm diameter by 30cm long cylindrical glass chamber to hold a dusty plasma that can be placed in a large solenoid to study the levitation and plasma densities of dense radioactive dusty plasmas. Several methods can be used to ionize and trap the dust, so that the experiment can operate in several different modes depending on pressure, dust composition, and plasma density. The experimental setup is schematically diagrammed in Figure 9. Water-cooled magnet coils surround a glass cylinder in which transparent electrodes (a) and (b) are used to make a Malmberg-Penning trap for non-neutral plasma. The neutral buffer gas is ionized by electrons emitted from electrode (d), using either thermal emission or photoemission. The central plasma column is confined in the potential well defined by (a) and (b),

which traps the dust. Alphas and fission fragments are collected by detector (f) where trapping efficiency is determined by radial profile of the spectrum. Flat plate electrodes (c) provide an alternate method of trapping dust, by imposing a vertical electric field to counter-act gravity. The two different techniques depend crucially on the neutral pressure, with high pressure favoring the DC electric field levitation, and low pressure favoring the Malmberg non-neutral plasma levitation.

3.3 Physics of Extracting Fission Fragments from a Dusty Plasma

The extraction of fission fragments depends on the column density along a typical FF trajectory, which will depend on three factors: the size of the dust grains, the strength of the magnetic field, and the average density of dust and gas within the dusty plasma.

Dust Grain size

The average stopping distance for fission fragments in fissile fuels is some 10's of microns. Therefore the smaller the fuel dust grain size, the higher the energy of exiting fission fragments. Figure 3 shows a table of average energy loss as a function of radius of dust grain. Below a diameter of 1 micron, nearly all the energy of the FF is retained. In addition, small dust grains have better cooling properties, with a larger surface to volume ratio. However, smaller dust grains lead to a smaller average dust density, and therefore a larger volume of dust is needed to provide the same mass fissile blanket. In addition, dust that is less than a micron becomes more difficult to handle because of its colloidal suspension in air. Therefore 1-5 micron dust is the range of dust sizes we think are optimum for the design.

Magnetic Field

We can assume that the fission fragments come out of the dust grains with a 2π steradian spherical distribution. In the absence of a magnetic field, we can integrate over the dust cloud and estimate the fraction exiting the end-caps of the cylindrical chamber, as well as the average density observed by those fragments and the resulting energy distribution. In a magnetic field, the parallel velocity remains unchanged, but the perpendicular velocity is rotated, so that a higher percentage of FF exit along the caps.

While several Tesla are needed to reduce the gyroradius of the FF to fit within the 8 cm diameter of our chamber, we can estimate the trapped fraction with much smaller magnetic field strengths. Since the percentage of exiting FF depends on magnetic field strength, with increasing B-field causing decreasing gyroradius, we can image the end cap solid-state detector of the previous experiment as a function of B-field to get a magnetic spectrometer determination of the flux and average energy of the extracted FF. That is, the longer path taken by a spiralling FF encounters more density than the direct path parallel to the B-field, and since the greater the integrated density, the lower the resultant energy, then a spectral characterization of the FF will also determine the average density and hence the path length. By changing the magnetic field strength, the path length changes as well as the pattern on the detector, which enable us to infer both the density of the intervening gas as well as the average FF energy as it exits the dust grain itself. This diagnostic can then predict the FF spectra extrapolated to the high B-field and low-pressure expected in a working fission fragment reactor.

Average Density

In addition, if the dust cloud doesn't fill the cylinder completely, but is limited to the central portion, than the spiralling FF will encounter dust less frequently, and increase the escape probability. Structuring the dust, then, will allow FF exiting at certain angles an almost unobstructed escape, and thereby permit fine-tuning of the FF beam. Since we don't expect this to be important until much later in the design of the fissile blanket, we will consider only two geometries, a minimal container size where the dusty plasma fills the vacuum vessel completely, and a more spacious design where the dusty plasma fills only the central third of the vacuum vessel.

4 Experimental Design

We will work closely with the Radiation Safety officer at NASA/MSFC to make sure that all of our experiments

comply with federal and state guidelines for the handling of radioactive materials. All the participants in these experiments will have received the appropriate safety training as required by NASA Safety. In addition, we will implement even more stringent controls to monitor the before and after conditions of the equipment to demonstrate that no radioactivity has leaked or increased during the experiments.

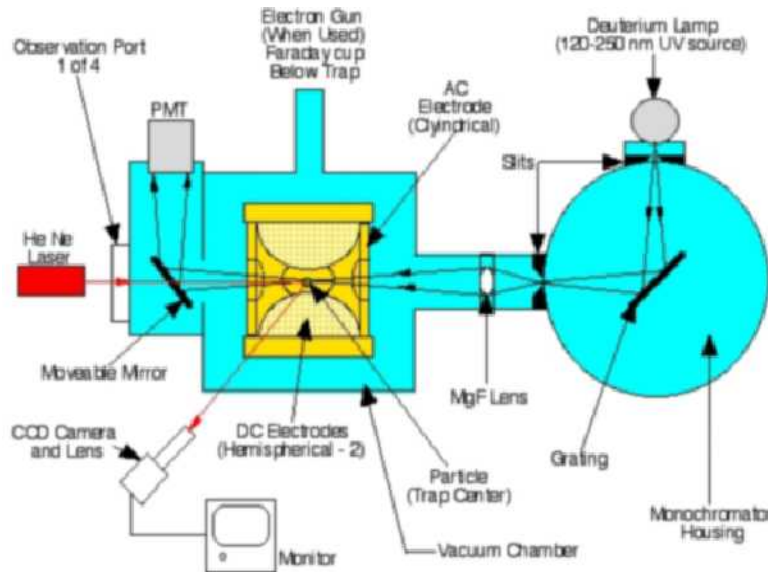


Figure 10: A schematic of the electrodynamic balance for dust.

4.1 Single Dust Grain Experimental Technique # 1

The experimental technique to be employed for measurements of discharging of radioactive micron/submicron size dust grains is based on a facility referred to as an electrodynamic balance (EDB) with the capability to conduct experiments on individual micron size dust grains in simulated space environments. Positively or negatively charged individual dust grains are inserted in a trap located in a small chamber where they are levitated in a potential well formed by hemispherical top and bottom electrodes kept at DC potentials, and a ring electrode at an AC potential, see Figure 10. The experimental details and the basic equations employed in the measurements have been given in the references [27, 28, 29, e.g.]. This facility has been employed for measurements of radiation pressure and rotation of interstellar dust grains, photoelectric yields, and secondary electron yields by electron impact on individual dust grains, see Figure 11[16, 30, 31, e.g.].

Experimental Apparatus

The experimental apparatus employed in the measurements of dust charging by exposing levitated dust grains to low energy electrons is based on the following equipment:

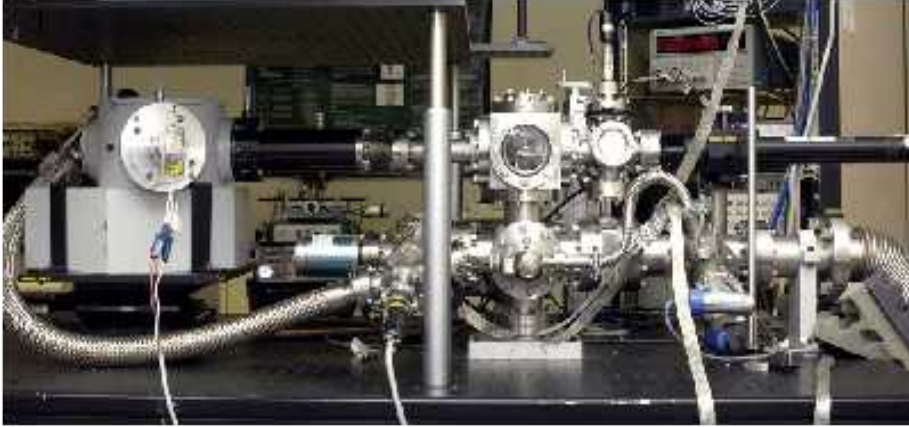


Figure 11: NASA/MSFC Dusty Plasma Lab showing electrodynamic balance, UV source and electron gun.

- (1) Electrodynamic Balance: consisting of top and bottom hemispherical electrodes with applied DC voltage V_{dc} and a ring electrode at an AC voltage of V at frequency
- (2) Electric Power Supplies: computer controlled for DC and AC potentials
- (3) Optical Equipment: for imaging a particle on a monitor, a 15 mW- He-Ne Laser, an optical imaging system with a CCD camera for projecting the levitated particle image on a monitor.
- (3a) Ultraviolet source based on a Deuterium lamp with a MgF window, a vacuum Monochromator with FWHM resolution of 8 nm, and an optical system to limit the beam diameter $\sim 3.5\text{--}4.5$ mm (FWHM) size, smaller than the entry/exit apertures of ~ 6 mm in the balance ring electrode thus minimizing any secondary electron emission from the walls excited by any stray UV radiation
- (3b) Photomultiplier tube (PMT) with a spectral response in the 115-200 nm wavelength region.
- (4) Low Energy Electron Gun: mounted at the top of EDB, with a power supply and controller for a selecting a mono-energetic Gaussian electron beam at desired energy levels.
- (5) A Faraday cup: below the EDB with an electrometer to measure the electron current.
- (6) Vacuum Equipment: to evacuate the system to pressures of torr.
- (7) Particle injector: A pressure impulse device to inject an inductively charged particle (positive or negative) of known composition and density in the balance through a port at the top.

Experimental Procedures

Positively or negatively charged particles are stably trapped in the EDB and the system is evacuated to pressures of 1-5 torr. The particle effective diameter D is determined by using the marginal stability conditions referred to as the "spring point method" [32, e.g.,] The system is then evacuated to pressures of torr, and the levitated particle exposed to an electron beam at selected energy levels in the 25--100 eV range. As the particle discharges or charges by electron impact, the particle position deviates from the trap center, requiring an adjustment in the DC voltage, $V(t)$ and providing a direct measurement of the particle charge $q(t)$ in accordance with,

$$(1)$$

where g is the gravitational acceleration, m is the particle mass, $r = 0.750$ cm is the distance from the trap center to the DC electrodes, k is a geometric constant determined experimentally as 0.68. With the determination of the effective particle diameter, the particle mass m is calculated by using the predetermined lunar dust grain mass density. Detailed descriptions of the experimental apparatus and the mathematical equations for evaluation of the measured quantities on an EDB have been given in previous publications [33, 34, 35, 17, 27, 16, 21, 28, 20, 30, 18, 31, 19, 36].

Experimental Protocols for Radioactivity

Backgrounds of the lab will be taken before the experiment. Chambers swabbed with cotton and alcohol, and tested

for radioactivity. Radioactive dust of ^{235}U , ^{241}Am , ^{32}Si , ^{60}Co , ^{22}Na and fissioning ^{252}Cf from IPL will be provided in glass syringes, which are thick enough to block all corpuscular radiation. The dust will either be cryomilled from bulk, or precipitated onto inert silicon dioxide dust, depending on whether it is delivered as a solid or a solution from IPL. Dilution will enable measurement of the effect of isotopic enrichment on the charging of dust grains, as well as a convenient way to adjust the range of curies per gram of the dust grains.

Test chambers are made of stainless steel, and will also block all radiation. Therefore the only exposure will be from samples that land on the bottom of the chamber. Upon the termination of the experiment, the chamber will be swabbed again with cotton and alcohol, and backgrounds measured as before. Should elevated radiation levels be found, the swabbing will be repeated with various solvents until values are at nominal background. All swabs and cleaning materials will be returned with the radioactive waste disposal procedures as determined by the radiation safety officer.

4.2 Dusty Plasma Experiment #2

This experiment will be conducted in the NASA/MSFC TOF Lab, with fume hood, vacuum chambers and access to missile grade GN2, compressed air, water and 3 phase power. Refer to figure 9 and 11b.

The facilities at MSFC dusty plasma lab can provide the lab space and vacuum pumps required. Non-boron glass cylinders of 3" diameter and 12" long will have transparent InSnO electrodes plated on the inside (c)(d) and outside (a)(b) to control the plasma. Because of its transparency, profiles of the dust density can be obtained optically. One of the end caps will have a silicon or cesium zinc telluride (CZT) particle detector (f) to obtain energy spectra of the radioactive particles, which will provide information on confinement and mean free path. The dust will be suspended and controlled either with a DC glow discharge plasma and self-ionizing radioactivity in the presence of variable strength magnetic fields.

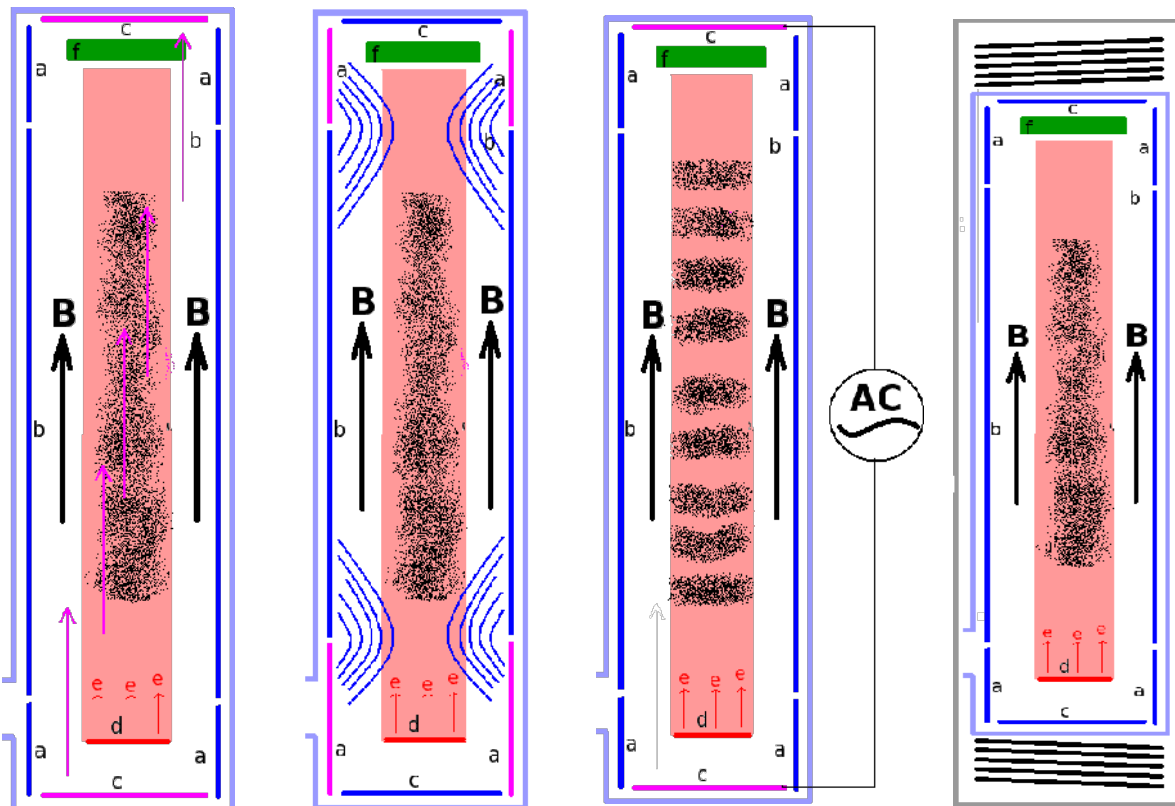


Figure 11. Panel 1 shows DC potentials on electrodes (c) that produce B-field aligned electric field to levitate dust. Panel 2 shows the DC potentials on electrodes (a) and (b) that electrostatically confine the dust through a non-neutral plasma, or virtual electrode. Panel 3 shows AC coupling on electrode (c) to change the dust distribution. Panel 4 shows a vibrating "shaker" with Cu-bronze spring for mechanical dust distribution.

Since the main purpose of this experiment is to demonstrate control of a dusty plasma, the various types of control are indicated in Figure 11b. Panel 1 shows the simple electric control obtained by placing a vertical capacitor whose electric field counteracts the force of gravity. It also drives a current through the plasma, heating it. This has been demonstrated at Auburn U, and operates at higher pressure, near the Paschen point.

Panel 2 demonstrates electrostatic control of the dust on electrodes (a) and (b). These fields compress the dust, by driving the ions to a small region of the experiment, effectively making a virtual anode in the center of the experiment much like the Polywell experiment. In addition, an AC voltage supplied to this radial field has been shown to provide a pondermotive force as in a Paul trap that can drive the dust to the center of the trap.

Panel 3 demonstrates AC control on electrode (c) which can set up dust acoustic waves in the plasma. Not only does this structure improve the extraction of fission fragments, but it may be possible to move packets of dust through the system, providing a way to continually replenish the fuel, and run the reactor in steady state. Higher frequency drivers may also interact with the ions, providing a way to manipulate the charge neutrality of the plasma.

Panel 4 demonstrates a mechanical "shaker" that would be implemented if the dust does not self-ionize, and it be found necessary to toss the dust into the center of the trap where the electron beam (from electron-emitting surface (d)) to ionize the dust. A voice coil attached to the inner glass container would drive the shaking, with Cu-bronze springs providing the restoring force.

Not shown are all the cables for these electrodes and detectors, which are snaked out through the vacuum manifold, and eventually through a vacuum feedthrough plate.

Ceramic (SmCo) magnets up to 0.001T, water-cooled magnets up to 0.1 T fields, and superconducting magnets up to 10T will be used to provide the background solenoidal field, and study its effects on the non-neutral plasma trapping, as well as the improved electrostatic trapping properties. Given the magnetic geometry, a 6" region near the center of the cylinder will have nearly uniform solenoidal magnetic field for comparison with theory. The water-cooled magnet can achieve magnetization of the hydrogen plasma, whereas the 10T superconducting magnet will achieve magnetization of even the fission fragments. The ceramic magnets, while not completely magnetizing the plasma, will permit insertion of the device into the 6" neutron beam tube needed for Experiment #3.

A highly filtered oil piston pump / turbopump combination, which can achieve kTorr to microTorr vacuum, will study the optimum neutral pressure for the various modes of trapping dusty plasma. Laboratory grade hydrogen, deuterium, argon and xenon will be used as a neutral buffer gas and for generating the plasma. A camera/laser combination will image the individual dust grains down the long axis of the plasma, to determine individual dust velocities, as is done at Auburn Univ [37, 38].

Radioactive dust clouds composed of ^{238}U , ^{235}U , ^{241}Am and ^{32}Si will be made by either cryomilling or precipitating onto 1-micron silicon dioxide dust, depending whether IPL provides the isotope as a solid or solution. Dilution on silicon dioxide dust will permit the determination of the critical radioactivity per gram needed to sustain a self-generated dusty plasma. Neither isotope of Uranium will have enough activity to self-charge, but they can be alloyed with radioactive isotopes to study their material properties and provide the experience for Experiment #3. Californium will not be tested due to expense and difficulty of handling the neutron emitter, but the results from Experiment #1 will be scaled with the results of ^{241}Am and ^{32}Si to estimate the parameters needed for the ^{235}U fission at a test reactor in Experiment #3. To provide continuity with previous non-radioactive dust experiments, and to test the properties of non-radioactive Uranium, we will either implement a "shaker" which consists of a Cu-bronze spring to mechanically lift dust from the bottom to the top to the chamber so as to allow electric charging of the falling dust, or we will alloy alpha-emitters sufficient to make the Uranium self-ionizing. The Uranium dust will be non-conductive UO_2 so that it does not short-out the electrodes in the chamber, or form metallic cold-welding in a vacuum.

Protocols for handling the ~ 1 micro-curie samples of radioactive dust will be similar to those for Experiment #1, with the additional precautions for handling the filters upstream of the pump. If necessary, Geiger counters and He3 neutron detectors can be used to monitor the experiment backgrounds, though fissioning is not expected to occur in this experiment.

Additional diagnostics include a high-speed color video camera combined with pulsed laser/diode light source so as to get stroboscopic videos of the dust grains, which can be analyzed for dust grain motions. Such an approach at Auburn University has been used to get acceleration and internal electric field measurements of the dusty plasma. Should the dust show evidence of overheating, an infrared spectroscope will be used to determine the surface temperature of the dust, and demonstrate radiative cooling (under electric current heating) of the dust. Faraday

rotation of the polarized light sources and/or Langmuir probes will be used to estimate plasma densities, floating potentials, and temperatures.

Appendix 1 lists the materials and vendors for this equipment.

4.3 Subcritical Nuclear Fission Experiment #3

This experiment will be conducted at the University of Florida Training Reactor (UFTR) facility. The purpose is three-fold: validating the levitation of dust in a fissioning, nuclear environment; validating the model of dust cooling through radiation; validating the extraction of fission fragments. Approximately 1g of fissile dust will be loaded into our glass test chamber as in Experiment #2, and placed in the water-cooled solenoid, or if necessary, the ceramic SmCo solenoid. The pressure and buffer gas composition will be set to those conditions determined from the previous experiment to be ideal for high density. A light source and remotely controlled camera will image the system, as well as a pyrometer, thermistors and particle detectors. The entire system will then be lowered into the 6" outer diameter south beam hole of the UFTR. At a distance of 12", the furthest extent of the experiment, Figure 13 gives a thermal neutron flux of ~10,000 neutrons/watt. We expect to run at about 10 MW power levels, which will provide 10^{11} thermal neutrons/cm², or about 10 decays/second on a UO₂ 4-micron dust-grain as simulated by the MNCP code. This should be a high enough charging rate for the dust to self-levitate, but if not, we can employ the shaker to mechanically separate the dust, and use electron beam ionization as was done at the University of Iowa Q-machine.

Once the dust is charged, it can be levitated and controlled by the electrostatic voltages, and the reactor power reduced (if necessary) to permit steady-state conditions. The dust density will be monitored with the video camera, and adjustments made to the levitating potentials of the electrodes in the system to keep the dust confined. The temperature and radiative heat dissipation as a function of reactor power and Joule heating can be ascertained with the IR spectrometer and thermistors. Since the MNCP simulation suggests that less than a watt of power is generated in the dust, the test will not directly evaluate the ability of dust to dissipate nuclear heating. However by increasing the heat load from Joule heating of the plasma, while simultaneously bombarding it with neutrons and gammas, we can obtain data for dust trapping under the conditions of a working dust reactor.

The extraction of fission fragments is the final goal of this experiment. Whereas a superconducting magnet will be needed to completely magnetize the FF, we can still achieve partial magnetization with a water-cooled magnet, and by calibrating the changes in the FF pattern on the SSD caused by B-fields in experiment #2, the pattern on the CZT particle detector can be used to monitor the FF density as a function of neutron flux. From this imaged, particle spectral measurement, the mean free path and magnetization of the FF can be deconvolved, and operational parameters of a working dusty plasma reactor calculated. In addition, since the gyrofrequency of the FF is about 1 GHz, whereas the plasma is likely to be transparent at those frequencies, it may be possible to use dynamic RF techniques to control the FF without disturbing the dust cloud. This would allow focussing and extraction of FF for increased electrical efficiency of a dusty reactor. Since the potential benefits are high, we include some RF diagnostics of the dusty plasma, looking for interaction with the CZT detector.

In conclusion, if the levitation and cooling properties of a fissioning dusty plasma are demonstrated along with the efficient extraction of fission fragments, then a working dusty plasma reactor can be designed.

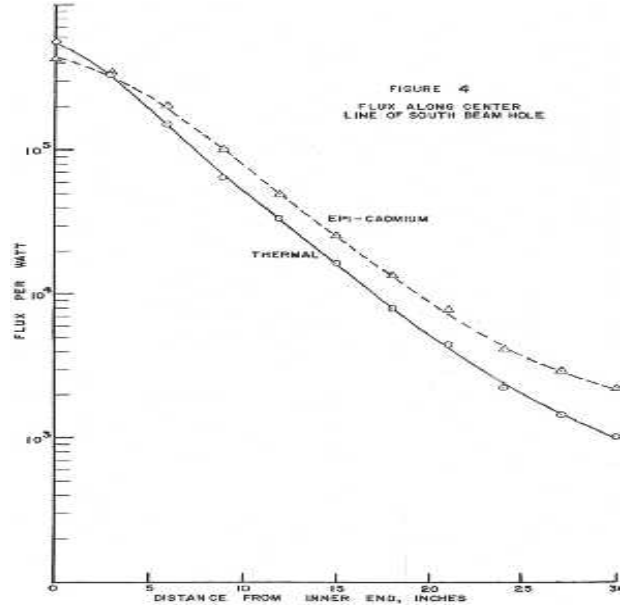


Figure 13: a) UFTR core after conversion to LEU. b) Neutron flux per watt of test reactor power along south beam hole

5 Conclusions

There are many advantages to a fusion nuclear reactor as discussed by Hans Bethe in 1979, in addition to the recent interest in finding a way to dispose of spent nuclear fuel. Burying it in the ground ignores its real potential as an almost unlimited source of raw material for producing additional fuel, without necessarily posing a proliferation risk. The major technological hurdles to a viable fusion reactor have been the success of fusion experiments, the power needed to generate fusion, and the heat dissipated in the fissile blanket. Recent advances in hydrogen fusion combined with the advantages of dusty plasma fissile feedback, permit the technological realization of a fusion reactor. We propose to study the physics of dusty plasma fission in order to understand the scaling from laboratory results to a self-sustaining dusty plasma fission reactor.

References

1. R. Clark and R. Sheldon, "Dusty Plasma Based Fission Fragment Nuclear Reactor", *AIAA Paper 2005-4460* (2005).
 2. G. Chapline, W. Howard, and B. Schnitzler, "Fission Fragment Rockets – a New Frontier" in 50 Years with Nuclear Fission ed. J. Behrens and A. Carlson, *American Nuclear Society* (1989).
 3. G. Chapline and Y. Matsuda, "Energy production using fission fragment rockets", *Fusion Technology* 20, 719 (1991)
 4. V. Fortov et. al. "Dust grain charging in a nuclear-induced plasma", *Phys. Lett. A284*, 118 (2001).
- [1] Clark, R. L. and Sheldon, R. B., "Dusty Plasma Based Fission Fragment Nuclear Reactor," *Proc. of 41st AIAA/ASME/SAE/ASEE JPC*, , No. AIAA-2005-4460, 2005.
 - [2] Thomas, E. and Watson, M., "First experiments in the Dusty Plasma Experiment device," *Physics of Plasmas*, Vol. 6, Oct. 1999, pp. 4111–4117.
 - [3] Ji, H., Betti, R., Drake, P., Goodman, J., Kronberg, P., Quataert, E., Stone, J., Uzdensky, D., Carter, T., Forest, C., Intrator, T., Li, H., Liang, E., Prager, S., Remington, B., Ryutov, D., Thomas, E., and Yamada, M., "Roles, Current Status, Opportunities, Future Trends, and Funding Issues for Laboratory Plasma Astrophysics," *Astronomy*, Vol. 2010, 2009, pp. 25P–+.
 - [4] Feder, T., "Need for clean energy, waste transmutation revives interest in hybrid fusion–fission reactors," *Physics Today*, Vol. 62, No. 7, 2009, pp. 070000–+.

- [5] Bethe, H. A., "The fusion hybrid," *Physics Today*, Vol. 32, May 1979, pp. 44–.
- [6] Hirsch, R., "Inertial-Electrostatic Confinement of Ionized Fusion Gases," *Journal of Applied Physics*, Vol. 38, 1967.
- [7] Krall, N. A. and Bussard, R. W., "Forming and maintaining a potential well in a quasispherical magnetic trap," *Physics of Plasmas*, Vol. 2, No. 1, 1995.
- [8] Kesner, J., Garnier, D. T., Hansen, A., Mael, M., and Bromberg, L., "Helium catalysed D D fusion in a levitated dipole," *Nuclear Fusion*, Vol. 44, Jan. 2004, pp. 193–203.
- [9] El-Wakil, M. M., *Nuclear Energy Conversion*, Intext Educational Publishers, Scranton, PA 18515, 2002.
- [10] Interaction, M. C. N. P., 2005.
- [11] Shulkla, P. K. and Mamun, A. A., *Introduction to Dusty Plasma Physics*, Series in Plasma Physics, Institute of Physics Publishing Ltd, Philadelphia, 2002.
- [12] Fortov, V. E., Nefedov, A. P., Vladimirov, V. I., Deputatova, L. V., Molotkov, V. I., Rykov, V. A., and Khudyakov, A. V., "Dust particles in a nuclear-induced plasma," *Physics Letters A*, Vol. 258, July 1999, pp. 305–311.
- [13] Sheldon, R., E. Thomas, J., Abbas, M., Gallagher, D., Adrian, M., and P. Craven, "Dynamic and Optical Characterization of Dusty Plasmas for Use as Solar Sails," *Space Technology and Applications International Forum-STAIF 2002*, edited by M. S. El-Genk, AIP, 2002.
- [14] Sheldon, R. B. and Spurrier, S., "The Spinning Terrella Experiment: Initial Results," *Physics of Plasmas*, Vol. 8, No. 4, 2001, pp. 1111–1118.
- [15] Draine, B. and Salpeter, E. E., "On the Physics of Dust Grain Charging in Hot Gas," *The Astrophysical Journal*, Vol. 231, July 1979, pp. 77–94.
- [16] Abbas, M. M., Craven, P. D., Spann, J. F., Spann, J. F., Tankosic, D., Leclair, A., Witherow, W. K., Camata, R., and Gerakines, P., "Laboratory Measurements of Optical Properties of Micron Size Individual Dust Grains," *Astrophysics of Dust*, 2003.
- [17] Abbas, M. M., Craven, P. D., Spann, J. F., West, E., Pratico, J., Tankosic, D., and Venturini, C. C., "Photoemission Experiments for Charge Characteristics of Individual Dust Grains," *Physica Scripta Volume T*, Vol. 98, 2001, pp. 99–103.
- [18] Abbas, M., Tankosic, D., Craven, P., Hoover, R., Taylor, L., Spann, J., Leclair, A., and West, E., "Laboratory Measurements of Optical and Physical Properties of Individual Lunar Dust Grains," *36th COSPAR Scientific Assembly*, Vol. 36 of *COSPAR, Plenary Meeting*, 2006, pp. 3238–.
- [19] Abbas, M. M., Tankosic, D., Craven, P. D., Hoover, R. B., Taylor, L. A., Spann, J. F., Leclair, A., and West, E. A., "Measurements of Photoelectric Yields of Individual Lunar Dust Grains," *Dust in Planetary Systems*, Vol. 643, Jan. 2007, pp. 165–170.
- [20] Abbas, M., Craven, P., Spann, J., Tankosic, D., Leclair, A., Gallagher, D., West, E., Weingartner, J., and Witherow, W., "Laboratory experiments on rotation of micron size cosmic dust grains with radiation," *35th COSPAR Scientific Assembly*, Vol. 35 of *COSPAR, Plenary Meeting*, 2004, pp. 3040–.
- [21] Abbas, M. M., Craven, P. D., Spann, J. F., Witherow, W. K., West, E. A., Gallagher, D. L., Adrian, M. L., Fishman, G. J., Tankosic, D., LeClair, A., Sheldon, R., and Thomas, E., "Radiation pressure measurements on micron-size individual dust grains," *Journal of Geophysical Research (Space Physics)*, Vol. 108, June 2003, pp. 1229–.
- [22] Sato, N., Uchida, G., Kaneko, T., Shimizu, S., and Iizuka, S., "Dynamics of fine particles in magnetized plasmas," *Physics of Plasmas*, Vol. 8, May 2001, pp. 1786–1790.
- [23] Sheldon, R., Gallagher, D., Adrian, M., Abbas, M., Craven, P., and Thomas, E., "Electromagnetically trapped dusty plasma ring," *34th COSPAR Scientific Assembly*, Vol. 34 of *COSPAR, Plenary Meeting*, 2002.
- [24] Malmberg, J. H., Driscoll, C. F., Beck, B., Eggleston, D. L., Fajans, J., Fine, K., Huang, X.-P., and Hyatt, A. W., "Experiments with pure electron plasmas," *American Institute of Physics Conference Series*, Vol. 175 of *American Institute of Physics Conference Series*, Nov. 1988, pp. 28–74.
- [25] Tiouririne, T. N., Turner, L., and Lau, A. W. C., "Multipole traps for non-neutral plasmas," *Physical Review Letters*, Vol. 72, Feb. 1994, pp. 1204–1207.
- [26] Fajans, J., "Non-neutral plasma equilibria, trapping, separatrices, and separatrix crossing in magnetic mirrors," *Physics of Plasmas*, Vol. 10, May 2003, pp. 1209–1214.
- [27] Abbas, M. M., Craven, P. D., Spann, J. F., Tankosic, D., Leclair, A., West, E., Sheldon, R., Witherow, W. K., Gallagher, D. L., Adrian, M. L., Fishman, G. J., Fix, J. D., Horayani, M., Mann, I., Mendis, D. A., Nuth, J. A.,

- and Rosenberg, M., "Laboratory Studies of the Optical Properties and Condensation Processes of Cosmic Dust Particles," *NASA Laboratory Astrophysics Workshop*, edited by F. Salama and et al., Nov. 2002, pp. 180–+.
- [28] Abbas, M. M., Craven, P. D., Spann, J. F., Tankosic, D., LeClair, A., Gallagher, D. L., West, E. A., Weingartner, J. C., Witherow, W. K., and Tielens, A. G. G. M., "Laboratory Experiments on Rotation and Alignment of the Analogs of Interstellar Dust Grains by Radiation," *The Astrophys. J.*, Vol. 614, Oct. 2004, pp. 781–795.
- [29] Abbas, M. M., Tankosic, D., Spann, J. F., Leclair, A., Dube, M. J., and Gaskin, J. A., "Experimental Studies of Electrostatic Charging of Individual Lunar Dust Grains by Photoelectric Emissions and by Electron Impact," *LPI Contributions*, Vol. 1415, July 2008, pp. 2033–+.
- [30] Abbas, M. M., Tankosic, D., Craven, P. D., Spann, J. F., LeClair, A., West, E. A., Weingartner, J. C., Tielens, A. G. G. M., Nuth, J. A., Camata, R. P., and Gerakines, P. A., "Photoelectric Emission Measurements on the Analogs of Individual Cosmic Dust Grains," *The Astrophys. J.*, Vol. 645, July 2006, pp. 324–336.
- [31] Abbas, M. M., Tankosic, D., Craven, P. D., Spann, J. F., Leclair, A., and West, E. A., "Lunar dust charging by photoelectric emissions," *Planetary and Space Science*, Vol. 55, May 2007, pp. 953–965.
- [32] Davis, E. J., "The electrodynamic balance for microparticle characterization," *Langmuir*, Vol. 1, 1985, pp. 379–387.
- [33] Ward, T. L., Davis, E. J., Jenkins, Jr., R. W., and McRae, D. D., "Electrodynamic radioactivity detector for microparticles," *Review of Scientific Instruments*, Vol. 60, March 1989, pp. 414–421.
- [34] Davis, E. J., Buehler, M. F., and Ward, T. L., "The double-ring electrodynamic balance for microparticle characterization," *Review of Scientific Instruments*, Vol. 61, April 1990, pp. 1281–1288.
- [35] Spann, J. F., Abbas, M. M., Venturini, C. C., Venturini, C. C., and Comfort, R. H., "Electrodynamic Balance for Studies of Cosmic Dust Particles," *Physica Scripta Volume T*, Vol. 89, 2001, pp. 147–153.
- [36] Abbas, M. M., Tankosic, D., Spann, J. F., Dube, M. J., and Gaskin, J. A., "Measurements of Charging of Apollo 17 Lunar Dust Grains by Electron Impact," *Space Technology and Applications International Forum-STAIF 2008*, edited by M. S. El-Genk, Vol. 969 of *American Institute of Physics Conference Series*, Jan. 2008, pp. 942–948.
- [37] Thomas, E., "Direct measurements of two-dimensional velocity profiles in direct current glow discharge dusty plasmas," *Physics of Plasmas*, Vol. 6, July 1999, pp. 2672–2675.
- [38] Thomas, E. and Williams, J., "Applications of stereoscopic particle image velocimetry: Dust acoustic waves and velocity space distribution functions," *Physics of Plasmas*, Vol. 13, No. 5, May 2006, pp. 055702–+.
- [39] ORLN, "Fact Sheet," "[http://www.sns.gov/hfir/hfir/s/do5\(t\)technical/s/do5\(p\)arameters.shtml](http://www.sns.gov/hfir/hfir/s/do5(t)technical/s/do5(p)arameters.shtml)", 2009.

Appendix I.

Parts List

Description	Vendor	Quantity	Cost/unit *	Total
Dust container				
1 Glass cylinder	ace	5	10 approx	50
	grayglass		quote coming?	0
2 Vacuum pump	available	1		0
3 ampule opener		5		0
4 Cu plates	available	5	\$10	\$50
5 Glass blowing	custom	5	\$100 per hour	\$500
6 Getter	Ref 2 SAES	5	n/a for hydrogen!	0
7 InO conductors	reynard	1	\$1,150	\$1,150
gold plating solution	american		\$200	\$0
Diagnostics				
1 Hi frame video	StreamviewBasler	1	\$3,000 6000 hi-res	\$3,000
2 532 nm laser	laserglow	1	\$200	\$200
3 Spectrometer/pyrometer	omega	1	\$200	\$200
4 Optical lenses/mounts	Edmund	5	\$100	\$500
5 Alpha/fission detector	sg	1	\$500 need a quote	\$500
6 SSD using CZT	Quickpak	1	\$1,000 need a quote	\$1,000
7 Langmuir probes	homemade	10	\$100	\$1,000
8 Pressure gauge		5	\$100	\$500
9 Thermistors	Digikey	25	\$100	\$2,500
Magnet				
1 Cu Magnet coil	E. McGrath	1	\$4,000 homebuilt, \$9k cust	\$4,000
2 Magnet power supply	GMW assoc	1	\$6,000	\$6,000
3 Magnet water pump/chiller	GMW assoc	1	\$6,000	\$6,000
4 Superconducting magnet	HTC110	1	\$250,000 quote coming	\$250,000
5 NdFeB Magnets	mce	1	quote coming?	0
	k&J	8	\$95 (3"D,2"d,1"w)=6kG	\$760
Analysis				
1 PIV hardware	LaVision	1	\$20,000 homebuilt, 100k cor	\$20,000
2 Computer	WWW	1	\$3,000	\$3,000
3 Labview interface+software	GMW assoc	1	\$2,000	\$2,000
4 PHA	OR/Canberra	1	\$10,000	\$10,000
5 SSD amp/discr	OR/Canberra	1	\$5,000	\$5,000
6 Langmuir Probe electronics	various	1	\$200	\$200
7 Oscilloscope	Techtronix	1	\$2,000	\$2,000
Supplies				
1 Cf 252 alpha+fission	IPL	1	quote coming?	0
2 Am 241 alpha	IPL	1	quote coming?	0
3 Si 32 beta	IPL	1	quote coming?	0
4 Co 60 gamma	IPL	1	quote coming?	0
5 Na 22 positron	IPL	1	quote coming?	0
6 "mixed"	IPL	1	quote coming?	0
7 Precipitation chemicals	Fisher	3	\$100	\$300
8 Glassware	ace	4	\$200	\$800

* price sheets available on the web, rather than current price quote. May reflect a 2008 value.

Reference 1 "Fabrication of Low-Field Water-Cooled Resistive Magnets for Small Animal Magnetic Resonance Imagir

Totals

###

(all 5 \$321,210.00

